Scientific Research Publishing

Open Journal of Applied Sciences, 2026, 16(3), 798-811
https://www.scirp.org/journal/ojapps
ISSN Online: 2165-3925
ISSN Print: 2165-3917

Detection of Nitrate Ions in Water Using Carbon Quantum Dots Modified with Silver Nanoparticles Functionalized by Cysteine

Irié Bi Irié Williams[1,2*], Aka Alla Martin[1], Meledje Jean Claude[1], Loba Kokora Seraphin[1], Pomi Bi Boussou Narcisse[1], Koffi Koffi Kra Sylvestre[1]

[1]Laboratory of Constitution and Reaction of Matter, UFR SSMT, Université Felix Houphouet Boigny, Abidjan, Côte d'Ivoire
[2]Department of Science and Technology, Université Alassane Ouattara, Bouaké, Côte d'Ivoire
Email: *iriebiwilliams@uao.edu.ci

How to cite this paper: Williams, I.B.I., Martin, A.A., Claude, M.J., Seraphin, L.K., Narcisse, P.B.B. and Sylvestre, K.K.K. (2026) Detection of Nitrate Ions in Water Using Carbon Quantum Dots Modified with Silver Nanoparticles Functionalized by Cysteine. *Open Journal of Applied Sciences*, **16**, 798-811.
https://doi.org/10.4236/ojapps.2026.163049

Received: February 19, 2026
Accepted: March 13, 2026
Published: March 16, 2026

Abstract

This work presents a novel sensor for detecting nitrates in water using silver nanoparticles (AgNPs) modified with cysteine-functionalized carbon quantum dots (Cys-CQDs) reduced by sodium borohydride ($NaBH_4$). This colorimetric detection method demonstrated a visible color change from yellow to pink, responding to both high nitrate concentrations (160 - 800 mg/L) with a rapid response time and low concentrations (0 - 40 mg/L) within a 30-minute exposure. UV-Vis spectroscopy analysis revealed a broad detection range of 0.0251 to 800 mg/L using the absorption peak associated with AgNPs at 400 nm. A linear calibration curve with excellent correlation (R^2 = 0.9995) was established across this range. The developed sensor exhibited remarkable performance, with a detection limit of 2.5×10^{-2} mg/L, a quantification limit of 8.4×10^{-2} mg/L, a recovery rate exceeding of 97%, and high precision (<5% RSD). These results suggest that this sensor holds great potential for practical applications in water quality control and nitrate pollution monitoring, offering a simple, sensitive, and cost-effective solution for environmental analysis.

Keywords

Nitrate Detection, Colorimetric Sensor, Carbon Quantum Dots, Silver Nanoparticles, Water Monitoring

1. Introduction

Nitrates (NO_3^-) play a crucial role in aquatic ecosystems, serving as essential nutrients for phytoplankton and plants [1]. This process supports primary use by photosynthesis, thus linking the nitrogen cycle to the overall carbon cycle and in-

fluencing climate regulation [2]. However, excess nitrates, often resulting from anthropogenic discharges, can lead to eutrophication of aquatic environments, disrupting the ecological balance [3]. In addition to environmental problems, high nitrate concentrations in water pose major health risks, notably through the formation of nitrosamines and nitrosamides, which are carcinogenic compounds and can cause methemoglobinemia in infants and pregnant women [4]. Faced with these various problems, the U.S. Environmental Protection Agency (USEPA) and the World Health Organization (WHO) have established a maximum nitrate level in drinking water (WHO, 2017; USEPA, 2020). This limit is also in effect in Côte d'Ivoire, as stipulated by the NIT 09-01 standard (Ivorian Technical Standard) relating to the quality of drinking water, which sets the same limit of 50 mg/L for nitrate ions (NO_3^-) (Ministry of Water Resources, 2021).

To address these challenges, our study focused on the development of sensors based on cysteine-modified carbon quantum dots (CQDs). CQDs are synthesized from carbon precursors such as lemon powder, while cysteine, a sulfur-containing amino acid, serves as both a functionalizing agent (providing thiol-SH and amine -NH_2 groups) and a passivating agent [5]. This modification confers upon the CQDs a particular affinity for metal ions and anions such as nitrates.

In a complementary approach, we also explored the formation of Cys-CQDs/AgNPs nanocomposites, where silver nanoparticles (AgNPs) are generated *in situ*. This hybrid system combines the optical properties of CQDs with the plasmonic effects of AgNPs, offering interesting prospects for improving detection performance [6].

This study builds upon recent work on functionalized nanomaterials for environmental detection [7], while proposing an innovative approach combining the advantages of CQDs and AgNPs for more sensitive and selective nitrate detection in water.

2. Materials and Methods

2.1. Reagents

All reagents used in this study were of analytical grade. The products used were: L-cystine (98%), silver nitrate ($AgNO_3$, 99%), anhydrous sodium carbonate (Na_2CO_3, 99%), sodium chloride (NaCl, 98%), magnesium chloride ($MgCl_2$, 98%), calcium chloride ($CaCl_2$, 99%), sodium hydroxide (NaOH, 98%), and sodium borohydride ($NaBH_4$, 99%), supplied by Sigma Aldrich. Lemon powder, obtained by grinding lemon peel, was purchased commercially.

A grinder equipped with a robust JIASOUNG JS8000 C motor, with a power rating of 3000 W, a frequency of 50 Hz, and a maximum speed of 5 rpm, was used to obtain the lemon powder. A high-speed benchtop centrifuge from the company MRCLTD with a maximum capacity of 13,000 rpm, set at 4000 rpm, was also used for all centrifugation operations. UV-Vis spectral curves were recorded using an Ocean Optics FLAME spectrophotometer (USA). Fluorescence measurements of the CQDs were performed using a UV lamp with two wave-

lengths (254 and 365 nm). The demineralized water used in this work came from the water purification system of Sichuan Zhuoyue Water Treatment Equipment CO., Ltd. (Chengdu, China). This system produces demineralized water with a resistivity of 18.25 MΩ·cm.

2.2. Sensor Synthesis

The sensor was manufactured in three (3) main steps:

Step 1: Hydrothermal Synthesis of Cys-CQDs

A lemon powder was prepared by calcining lemon pulp at 200˚C for 1 hour. 250 mg of this powder and 150 mg of L-cysteine were dissolved in 50 mL of deionized water. The mixture was then transferred to a Teflon reactor, sealed in a stainless steel autoclave, and heated at 180˚C for 12 hours. After cooling, the solution was centrifuged at 10,000 rpm for 15 minutes and then filtered through a 0.22 µm membrane to remove aggregates and obtain a pure aqueous suspension of Cys-CQDs.

Step 2: Cys-CQD Reduction

10 mL of the Cys-CQD suspension is mixed with 50 mg of sodium borohydride ($NaBH_4$) under magnetic stirring (500 rpm) at room temperature for 8 hours. The excess $NaBH_4$ was removed by centrifugation, thereby significantly minimizing the presence of residual borohydride in the final suspension. This step reduces the surface functional groups and increases the passivation of the CQDs.

Step 3: Functionalization of AgNPs with reduced Cys-CQDs

1 mL of reduced Cys-CQDs was dispersed in 200 mL of distilled water under magnetic stirring (600 rpm) for 2 minutes. 0.02 g of silver nitrate ($AgNO_3$) was added under stirring for an additional 2 minutes. The mixture was then heated to 70˚C for 30 minutes, and 0.1 g of sodium hydroxide (NaOH) was added. The reaction was activated under stirring on a hot plate (70˚C, 600 rpm) for 8 hours to allow the formation of Cys-CQDs/AgNPs nanocomposites via silver thiol bonding [8].

2.3. Colorimetric/UV-Vis Detection of Nitrate Ions

To two milliliters of standard solution (or water sample), 50 µL of the sensor solution is added, followed by 1 minute of homogenization. After homogenization, the color change of the mixture is monitored over time, and then the absorption spectrum is recorded. For quantitative analysis, the absorbance was recorded after a fixed incubation time of 3 min, corresponding to the plateau region of the kinetic response curve. The calibration curve is subsequently established under the same conditions with different concentrations of the nitrate ion standard solution (0, 4, 8, 16, 40, 160, 200, 640, and 800 mg/L), between the difference in absorbance (A0) in the absence and maximum absorbance (Ai) in the presence of nitrate ions at a wavelength 400 nm, relative to the nitrate ion concentrations ($A0 - Ai = f(C)$).

2.4. Validation Criteria for Analytical Methods

The validation of an analytical method is a procedure that establishes, through

experimental studies, that the method's performance criteria meet the requirements of its intended use. It is worth recalling that the objective of an analytical assay method is to quantify each unknown quantity that the analyst will have to evaluate as accurately and precisely as possible. The objective of validation, on the other hand, is to provide the laboratory and regulatory authorities with sufficient assurance that each measurement performed routinely with a given method will be close to the truth. At this stage, it is important to define some frequently encountered terms.

2.4.1. Linearity

The linearity range represents the concentration range explored during method validation. This range must take into account all possible future results. Indeed, if, during routine use of the method, the unknown quantities that the laboratory will have to measure fall outside the linearity range, the results provided will not be valid considered reliable. The linearity of an analytical procedure is its ability, within a certain titration range, according to a predefined mathematical function, to obtain the analyte concentration in the sample. Linearity in this study was verified by plotting absorbance against concentration. The limit of detection and quantification was also determined using this same calibration curve.

2.4.2. Limit of Detection

The limit of detection (LOD) is the smallest concentration or quantity of a parameter or analyte that produces a detectable signal with a defined reliability and is statistically different from that produced by a blank under the same conditions [9]. It is calculated using Equation (1):

$$LOD = 3 \times s / S \tag{1}$$

With s being the standard deviation of the deviation and S the slope of the calibration curve.

2.4.3. Limit of Quantification

The limit of quantification is the concentration equivalent to 10 times the standard deviation obtained when establishing the limit of detection of the method [10] as described by Equation (2).

$$LOQ = 10 \times s / S \tag{2}$$

It is also the smallest quantity of a substance to be examined in a sample that can be quantified under the described experimental conditions with an acceptable coefficient of variation of the response factor [11].

2.4.4. Accuracy

Accuracy, or recovery rate, or percentage recovery is the percentage difference between the measured concentration of a fortified sample and the measured concentration of the same unfortified sample, divided by the concentration of the added substance. This ratio takes into account any chemical transformation that has occurred. This rate is expressed by Equation (3).

$$Recovery\ rate(\%) = 100 \times \left(C_f - C/C_a\right) \quad (3)$$

where C_f: Measured concentration of the fortified sample; C: Measured concentration of the unfortified sample; C_a: Concentration of the added substance.

2.4.5. Precision

Precision expresses the closeness of agreement (degree of dispersion, coefficient of variation) between a series of measurements taken from multiple aliquots of a homogeneous sample under the prescribed conditions [11]. It is generally expressed by the coefficient of variation (Cv in %), which is obtained by dividing the standard deviation (SD) of the test results by the mean of the observed responses (2) [12]. Precision reflects only the distribution of random errors and has no relation to the true or specified value. Quantitative measures of precision are critically dependent on the stipulated conditions.

2.4.6. Sensitivity

The sensitivity of an analytical procedure can be defined as the ratio of the change in the analytical method's response to the change in the amount of analyte. A procedure is considered sensitive if a small change in the concentration or amount of analyte results in a change in the response. In this study, sensitivity was verified by measuring the concentration of nitrate ions in the presence of other compounds that could interfere with its detection.

3. Results and Discussion

3.1. Characterization of the Synthesized Sensors

The different synthesized materials were analyzed by UV-Vis spectroscopy (**Figure 1**). First, the spectrum of Cys-CQDs (**Figure 1(a)**) shows a strong absorption picture at 242 nm. This peak is typical of π→π* electron transitions in aromatic carbon structures (sp^2 domains) that form during hydrothermal synthesis. A small shoulder is also observed around 320 nm, corresponding to n-π* transitions of heteroatoms such as carbonyl (C=O), amine, etc., groups on the surface. These two peaks are characteristic of carbon quantum dots. It should be noted that the presence of these heteroatoms contributes to the reactivity and passivation of CQDs. Furthermore, the spectrum of reduced Cys-CQDs (**Figure 1(b)**) shows changes at the shoulder at 320 nm. This

indicates that the surface groups have been modified, confirming that the reduction has worked well. This step was necessary to activate the reducing power of the CQDs. Finally, the spectrum of the Cys-CQDs/AgNPs nanocomposite (**Figure 1(c)**) is very revealing. It clearly shows the combination of the CQDs peak at 242 nm and a new, broad peak centered at 421 nm. This new peak is the signature of the silver nanoparticles (AgNPs): it is the surface plasmon resonance (SPR) phenomenon, which proves that the silver ions (Ag^+) were indeed reduced to metallic silver (Ag^0) by the Cys-CQDs, which in turn underwent oxidation. Thus, upon the addition of $AgNO_3$, the reduction of Ag^+ ions is primarily attributed to

the surface functional groups of CQDs-Cys (notably –OH, –COOH, and $–NH_2$), which can act as mild reducing and stabilizing agents. This good stability is essential for considering a reliable application as a sensor.

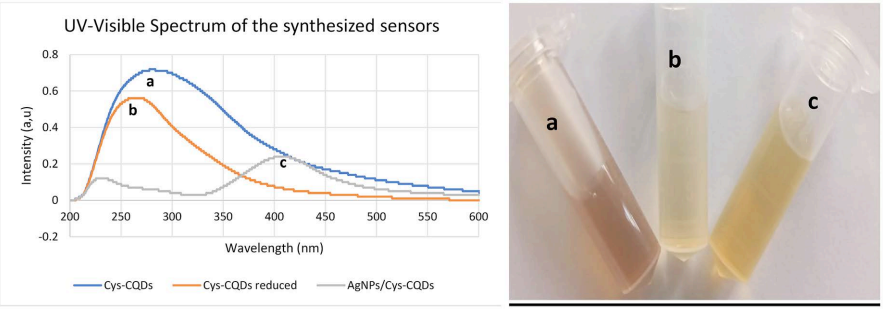

Figure 1. UV-Visible Spectrum of the synthesized sensors: (a) Cys-CQDs, (b) reduced Cys-CQDs, and (c) Cys-CQDs/AgNPs.

3.2. Study of Sensor Fluorescence

The study of photoluminescence properties revealed distinct behaviors for each nanomaterial (**Figure 2(B)**), providing crucial information on their structure and interactions. Cys-CQDs exhibit intense blue fluorescence under excitation at 365 nm. This strong emission results from the combination of two main mechanisms: the quantum confinement effect in nanometer-sized graphitic domains (sp_2), characteristic of CQDs [13], and the presence of heteroatoms (nitrogen, sulfur) from cysteine functionalization, which create surface electronic states amplifying light emission. For reduced Cys-CQDs, a significant increase in fluorescence intensity is observed. This improvement results from the reduction of carbonyl groups (C=O) to hydroxyl groups (–OH) by $NaBH_4$, thus decreasing the density of surface "non-radiative traps." This passivation promotes radiative recombination, leading to a higher quantum yield, consistent with the mechanisms described by Shi and colleagues [14]. The most striking result concerns the Cys-CQDs/AgNPs nanocomposite, which exhibits near-total quenching of fluorescence. This phenomenon confirms the formation of an intimate nanocomposite, likely explained by fluorescence resonance energy transfer (FRET). In this By this mechanism, Cys-CQDs (donors) transfer their excitation energy to AgNPs (acceptors) in

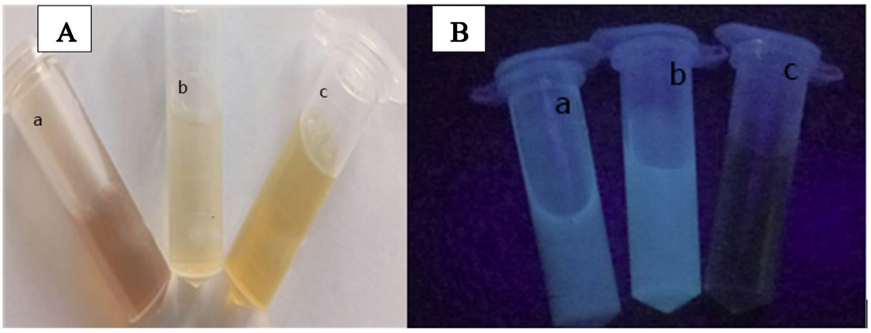

Figure 2. Fluorescence of synthesized sensors a) Cys-CQDs, b) reduced Cys-CQDs, and c) Cys-CQDs/AgNPs.

a non-radiative manner [15]. The efficiency of this transfer, which is highly dependent on distance (1 - 10 nm), confirms the close proximity between AgNPs and CQDs [6]. This fluorescence quenching is essential for sensor development, as analyte recognition could modulate this signal, thus generating a detectable response.

3.3. Demonstration of a Specific Colorimetric Response

A preliminary assessment of the nanomaterials' detector potential was performed using a simple colorimetric test. As shown in **Figure 3**, the solutions of Cys-CQDs (a, b) and reduced Cys-CQDs (c, d) showed no visible color change after the addition of nitrate ions (NO_3^-) compared to the controls in distilled water. In contrast, a clear positive response was observed for the Cys-CQDs/AgNPs nanocomposite. Its color changed from a pale yellow (tube e, control) to a distinctive pink (tube f) in the presence of nitrate. This preliminary result indicates that the Cys-CQDs/AgNPs nanocomposite is the only one among the materials tested to exhibit colorimetric sensitivity to nitrate ions, validating its selection for further investigation. This response suggests that this sensor can be used for the colorimetric detection of nitrates [16] [17]. Nitrate ions (NO_3^-) interact specifically with the sensor through the combined action of Cys-CQDs and AgNPs. The sensing response is likely associated with nitrate-induced modulation of the colloidal stability of AgNPs, possibly through ionic strength effects and electrostatic screening, leading to nanoparticle aggregation and consequent plasmonic changes. Similar behaviors have been reported in related AgNP-based sensing systems [18]-[20].

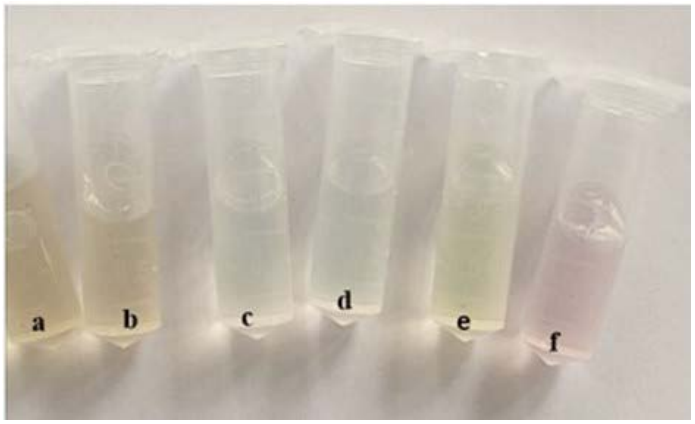

Figure 3. Solution of the synthesized sensors in the absence and presence of nitrate ions, respectively: (a), (b) Cys-CQDs, (c), (d) reduced Cys-CQDs, and (e), (f) Cys-CQDs/AgNPs.

3.4. Stability Study of the Selected Sensor

The stability of Cys-CQDs/AgNPs was investigated by recording the absorption spectra of the freshly prepared Cys-CQDs/AgNP colloidal solution after 1; 14; 30 and 60 days of synthesis (**Figure 4**).

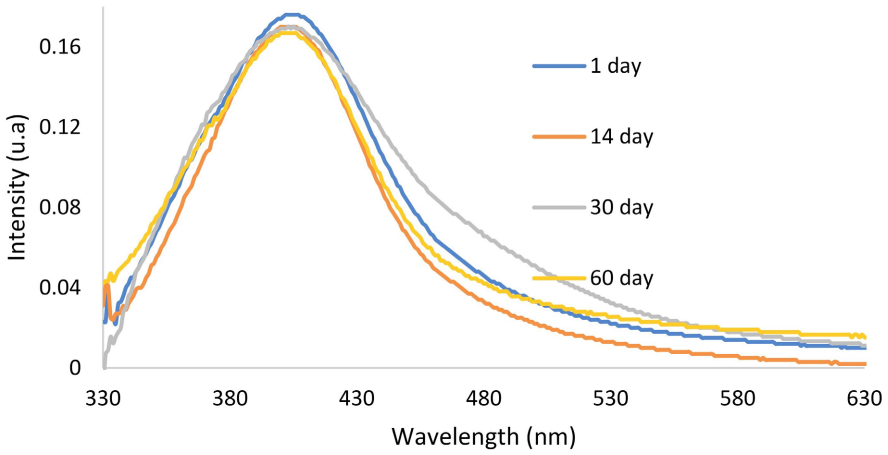

Figure 4. Stability of Cys-CQDs/AgNPs.

The absorbance of the colloidal Cys-CQDs/AgNPs solution, after 1, 14, 30, and 60 days of synthesis, exhibits the same absorption wavelength as that of the freshly prepared solution (400 nm). The results show that there is neither a significant decrease in the intensity of the absorbance peak nor a change in the position of the maximum wavelength, suggesting excellent stability of the prepared Cys-CQDs/AgNPs.

3.5. Detection

3.5.1. Calibration of the Detection Method

In order to determine the detection range of nitrate ions, different concentrations of the standard solution were evaluated (0; 4; 8; 16; 40; 160; 200; 640 and 800 mg/L) as shown in **Figure 5**.

The results indicate that the Cys-CQDs/AgNPs sensors exhibit a color change in the presence of nitrate ions. The color gradually changes from yellow to pink, intensifying over time and strongly dependent on the concentration. At high concentrations (160 - 800 mg/L), the pink coloration appears immediately. At low concentrations (4 - 40 mg/L), the complete change takes approximately 30 minutes. This encouraging visual observation motivated a more in-depth quantitative study. To this end, we established a calibration curve by measuring the change in absorbance (ΔA) as a function of concentration (**Figure 5(B)**).

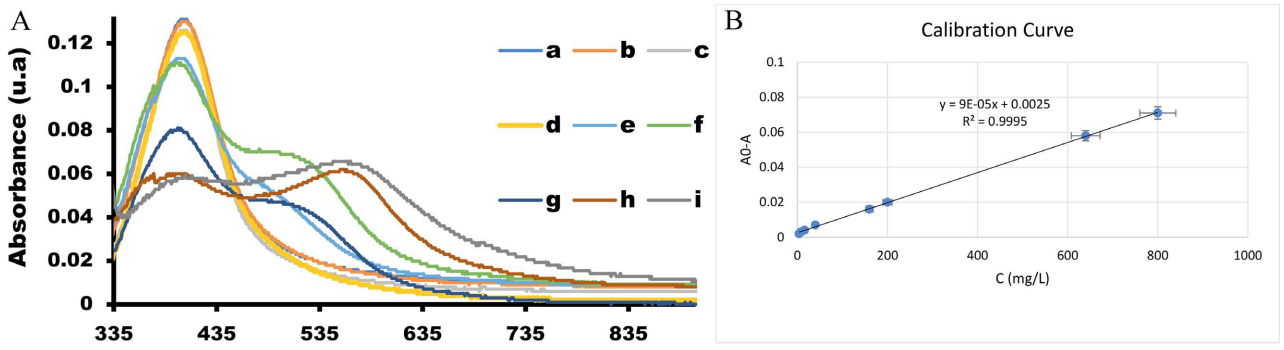

Figure 5. Calibration curve: (a) 0 mg/L, (b) 4 mg/L, (c) 8 mg/L, (d) 16 mg/L, (e) 40 mg/L.

The results obtained show a linear curve with Equation (4):

$$\Delta A = \left(9 \times 10^{-5}\right) \times \left[NO_3^-\right] + 0.0025 \quad (4)$$

The R^2 coefficient is 0.9995, extremely close to 1. This confirms that the relationship is not only linear but also highly reliable. Therefore, this equation can be used to determine the nitrate concentration of an unknown water sample simply by measuring the change in absorbance.

3.5.2. Limit of Detection and Quantification

The limits of detection and quantification were calculated using Equation (1) and Equation (2). The results obtained are LOD = 2.51×10^{-2} mg/L and LOQ = 8.38×10^{-2} mg/L. These results indicate that the sensor has an ultrasensitive detection capability, perfectly suited for environmental applications, as observed in other systems based on hybrid nanomaterials [21] [22].

3.5.3. Sensor Reliability

The sensor's reliability was evaluated through recovery rate experiments. Three (3) $NaNO_3$ solution samples at different concentrations were analyzed, with three (3) independent replicates for each. The results (**Table 1**) show recovery rates ranging from 97% to 104%, indicating excellent sensor reliability, in accordance with analytical criteria [23].

Table 1. Mean recovery rate and standard deviation (n = 3).

Introduced concentration (mg/L)	Found concentration (mg/L)	Recovery ± SD (%)
16	16.67	104.10 ± 0.007
40	38.89	97.22 ± 0.0007
120	116.66	97.00 ± 0.07

These results demonstrate that the Cys-CQDs/AgNPs sensor provides reliable measurements suitable for practical applications of monitoring nitrates in water.

3.5.4. Sensor Accuracy (Reliability)

The sensor accuracy was verified by inter-day and intra-day measurements of three (3) nitrate solution concentrations. Each concentration was measured three (3) times independently on the same day and on three (3) consecutive days. All values found (RSD) were less than 5% (**Table 2**). This high accuracy suggests that our chosen sensor can be used to detect nitrate ions.

Table 2. Relative recovery rate and standard deviation.

Introduced concentration (µg/mL)	Found concentration (µg/mL) RSD		RSD accuracy (%) (n = 3)	
	Intra-day ± SD	Inter-day ± SD	Intra-day	Inter-day
16	16.61 ± 0.070	16.63 ± 0.098	0.421	0.589
40	38.79 ± 0.012	38.80 ± 0.141	0.031	0.363
120	116.61 ± 0.071	116.63 ± 0.098	6.763	0.084

RSD: Relative Standard Deviation.

3.5.5. Interference Test on Nitrate Ion Detection by Our Sensor

Water contains many dissolved ions, the main ones being calcium (Ca^{2+}), magnesium (Mg^{2+}), sodium (Na^{+}), potassium (K^{+}), carbonates (CO_3^-), bicarbonates (HCO_3^-), sulfates (SO_4^{2-}), chlorides (Cl^-), and nitrates (NO_3^-). Therefore, compounds such as Na_2CO_3, NaCl, $MgCl_2$, and $CaCl_2$ were tested at concentrations 10 times higher than those of nitrate ions (NO_3^-) in the presence of our sensor to evaluate their interference with these different ions (Figure 6). The near 100% recovery rates confirm that variations in ionic strength do not affect the sensor's response [24]-[27].

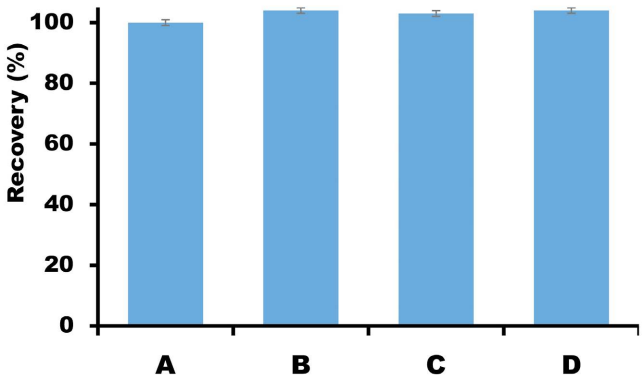

Figure 6. Recovery rates (A) of nitrate alone at 16 mg/L and of nitrate in the presence of 160 mg/L, including (B) NaCl, (C) $MgCl_2$, and (D) $CaCl_2$.

3.5.6. Nitrate Detection in the Real Matrix

To evaluate the effectiveness of the Cys-CQDs/AgNPs sensor under environmental conditions, water samples from wells, boreholes, lagoons, and taps were collected (2 mL each) and mixed with 50 µL of the Cys-CQDs/AgNPs nanocomposite. A distinct pink coloration was observed in all the tested matrix, visually confirming the presence of nitrate ions. Nitrate concentrations were then measured in each matrix (Table 3). The results show that the sensor effectively detects nitrates at both low and high concentrations, confirming its suitability for applications on complex environmental samples.

Table 3. Detection of nitrate in real matrix (n = 3).

matrix	Concentration (mg/L)
Tap water	16.6
Well water	66.66
Lagoon water	105
Borough water	94.44

These results confirm the effectiveness of nanomaterial-based sensors for the rapid and sensitive detection of nitrate ions in real water samples, consistent with previous work on environmental nitrate detection [28].

3.5.7. Comparison with Other Methods

To better illustrate the performance of the implemented technique, a comparison with results from the literature was conducted. The detection method, colorimetry using carbon quantum dots modified by silver nanoparticles (Cys-CQDs/AgNPs), showed a limit of detection (LOD) of 0.0251 mg/L, which is competitive with other methods. This colorimetric method is valued for its simplicity and efficiency, allowing direct visual detection without additional equipment [29]. Comparatively, other nitrate detection methods, such as high-performance liquid chromatography (HPLC), have higher limits of detection. For example, Uddin reported a limit of detection (LOD) of 2.26 mg/kg for nitrate determination in fruits and vegetables, which is significantly less sensitive than the Cys-CQDs/AgNPs method [30]. Furthermore, techniques such as flow injection analysis have also been used, with an LOD of 0.34 mg/kg, which is less effective than the aforementioned colorimetric method [31]. Other approaches, such as electrochemical sensors, have shown promising performance. For example, one study demonstrated that electrodes modified with palladium-gold nanoparticles detected nitrates with a sensitivity of 4.7 $\mu A \cdot mg^{-1} \cdot L$ [32]. However, these methods are hampered by more complex experimental conditions and heavy equipment. Furthermore, the systems Lab-on-a-chip devices have been developed for *in situ* analyses, achieving LODs of 0.025 µM, but they are generally more difficult to implement in the field [33]. In summary, the Cys-CQDs/AgNPs nitrate ion detection method with an LOD of 0.0251 mg/L is competitive with other techniques such as HPLC, flow injection analysis, and electrochemical sensors. Its simplicity, speed, and efficiency make it an attractive option for nitrate detection in various settings.

4. Conclusions

This work aimed to synthesize a new, simple, sensitive, and inexpensive chemical sensor for the detection of nitrate ions (NO_3^-) in water.

To achieve this objective, an innovative approach was adopted, based on the hydrothermal synthesis of cysteine-functionalized carbon quantum dots (Cys-CQDs) from agri-food waste (lemon peel), followed by their assembly with silver nanoparticles (AgNPs) to form a Cys-CQDs/AgNPs nanocomposite. Optical characterization (UV-Vis and fluorescence) confirmed the formation of the nanomaterials and revealed the synergistic interaction between the CQDs and the AgNPs, notably via energy transfer leading to fluorescence quenching. Real-world evaluation showed that the sensor reacts specifically to nitrate ions with a visible and distinct color change, shifting from yellow to pink, attributable to controlled aggregation of the silver nanoparticles induced by nitrate adsorption.

The analytical performance of the Cys-CQDs/AgNPs sensor is remarkable: it exhibits exceptional linearity ($R^2 = 0.9995$) over a wide detection range (0.0251 - 800 mg/L), covering both low natural concentrations and high levels of contamination. Its sensitivity is high, with a limit of detection (LOD) of 2.51×10^{-2} mg/L and a limit of quantification (LOQ) of 8.38×10^{-2} mg/L, well below the regulatory

threshold of 50 mg/L. Reliability and accuracy are confirmed by coefficients of variation (RSD) of less than 5% and recovery rates close to 100%. The sensor also shows notable selectivity towards common ions present in natural waters, minimizing the risks of interference, and its validation on real matrices (well water, borehole, lagoon and tap water) demonstrates its practical potential for environmental monitoring.

Conflicts of Interest

The authors declare no conflicts of interest regarding the publication of this paper.

References

[1] Wetzel, R.G. (2001) Limnology: Lake and River Ecosystems. Gulf Professional Publishing. https://books.google.ci/books?id=no2hk5uPUcMC&dq

[2] Falkowski, P., Scholes, R.J., Boyle, E., Canadell, J., Canfield, D., Elser, J., *et al.* (2000) The Global Carbon Cycle: A Test of Our Knowledge of Earth as a System. *Science*, **290**, 291-296. https://doi.org/10.1126/science.290.5490.291

[3] Smith, V.H., Tilman, G.D. and Nekola, J.C. (1999) Eutrophication: Impacts of Excess Nutrient Inputs on Freshwater, Marine, and Terrestrial Ecosystems. *Environmental Pollution*, **100**, 179-196. https://doi.org/10.1016/s0269-7491(99)00091-3

[4] Ward, M., Jones, R., Brender, J., De Kok, T., Weyer, P., Nolan, B., *et al.* (2018) Drinking Water Nitrate and Human Health: An Updated Review. *International Journal of Environmental Research and Public Health*, **15**, Article 1557. https://doi.org/10.3390/ijerph15071557

[5] Luo, H., Papaioannou, N., Salvadori, E., Roessler, M.M., Ploenes, G., van Eck, E.R.H., *et al.* (2019) Manipulating the Optical Properties of Carbon Dots by Fine-Tuning Their Structural Features. *ChemSusChem*, **12**, 4432-4441. https://doi.org/10.1002/cssc.201901795

[6] Zhang, Q., Du, S., Tian, F., Long, X., Xie, S., Tang, S., *et al.* (2022) Silver Nanoparticle-Functionalised Nitrogen-Doped Carbon Quantum Dots for the Highly Efficient Determination of Uric Acid. *Molecules*, **27**, Article 4586. https://doi.org/10.3390/molecules27144586

[7] Kra Sylvestre, K.K., Li, D., Kouadio Fodjo, E., Martin, A.A., Boussou Narcisse, P.B. and Irié Williams, I.B. (2025) Fast Detection of Melamine Using Silver Nanoparticles Capped with l-Cysteine Functionalized Carbon Dots. *RSC Advances*, **15**, 32031-32040. https://doi.org/10.1039/d5ra03280f

[8] Liu, M.L., Chen, B.B., Li, C.M. and Huang, C.Z. (2019) Carbon Dots: Synthesis, Formation Mechanism, Fluorescence Origin and Sensing Applications. Green Chemistry, **21**, 449-471. https://doi.org/10.1039/c8gc02736f

[9] Ienco, A., Mealli, C. and Dodoff, N.I. (2002) Synthesis and Structure of the First Transition Metal Complex with Methanesulfonylhydrazine as a Ligand. *Zeitschrift für Naturforschung B*, **57**, 865-867. https://doi.org/10.1515/znb-2002-0804

[10] Duwensee, H., Adamovski, M. and Flechsig, G. (2007) Adsorptive Stripping Voltammetric Detection of Daunomycin at Mercury and Bismuth Alloy Electrodes. *International Journal of Electrochemical Science*, **2**, 498-507. https://doi.org/10.1016/s1452-3981(23)17090-8

[11] Bicak, N. and Karagoz, B. (2008) Copper Patterned Polystyrene Panels by Reducing of Surface Bound Cu (II)-Sulfonyl Hydrazide Complex. *Surface and Coatings Tech-*

nology, **202**, 1581-1587. https://doi.org/10.1016/j.surfcoat.2007.06.040

[12] Mohamed, R. and Leong, W.L. (2006) Analysis of Selenium Species Using Cathodic Stripping Voltammetry. *Jurnal Teknologi* (*Sciences & Engineering*), **44**, 55-66.

[13] Li, L. and Dong, T. (2018) Photoluminescence Tuning in Carbon Dots: Surface Passivation or/and Functionalization, Heteroatom Doping. *Journal of Materials Chemistry C*, **6**, 7944-7970. https://doi.org/10.1039/c7tc05878k

[14] Shi, W., Li, X. and Ma, H. (2012) A Tunable Ratiometric pH Sensor Based on Carbon Nanodots for the Quantitative Measurement of the Intracellular pH of Whole Cells. *Angewandte Chemie International Edition*, **51**, 6432-6435. https://doi.org/10.1002/anie.201202533

[15] Chen, Y., Qin, X., Yuan, C. and Wang, Y. (2020) Switch on Fluorescence Mode for Determination of l-Cysteine with Carbon Quantum Dots and Au Nanoparticles as a Probe. *RSC Advances*, **10**, 1989-1994. https://doi.org/10.1039/c9ra09019c

[16] Rai, P., Mehrotra, S., Gautam, K., Verma, R., Anbumani, S., Patnaik, S., *et al.* (2024) A Polylactic Acid-Carbon Nanofiber-Based Electro-Conductive Sensing Material and Paper-Based Colorimetric Sensor for Detection of Nitrates. *Analytical Methods*, **16**, 3131-3141. https://doi.org/10.1039/d3ay02069j

[17] Mura, S., Greppi, G., Roggero, P.P., Musu, E., Pittalis, D., Carletti, A., *et al.* (2015) Functionalized Gold Nanoparticles for the Detection of Nitrates in Water. *International Journal of Environmental Science and Technology*, **12**, 1021-1028. https://doi.org/10.1007/s13762-013-0494-7

[18] Bélteky, P., Rónavári, A., Igaz, N., Szerencsés, B., Tóth, I.Y., *et al.* (2019) Silver Nanoparticles: Aggregation Behavior in Biorelevant Conditions and Its Impact on Biological Activity. *International Journal of Nanomedicine*, **14**, 667-687. https://doi.org/10.2147/ijn.s185965

[19] Yuan, B., Shangguan, S. and Zhao, D. (2024) Influence of Anions on the Antibacterial Activity and Physicochemical Properties of Different-Sized Silver Nanoparticles. *Molecules*, **29**, Article 4099. https://doi.org/10.3390/molecules29174099

[20] Lodeiro, P., Achterberg, E.P., Pampín, J., Affatati, A. and El-Shahawi, M.S. (2016) Silver Nanoparticles Coated with Natural Polysaccharides as Models to Study AgNP Aggregation Kinetics Using UV-Visible Spectrophotometry Upon Discharge in Complex Environments. *Science of the Total Environment*, **539**, 7-16. https://doi.org/10.1016/j.scitotenv.2015.08.115

[21] Khorablou, Z., Asadian, E., Shahdost-Fard, F., Zarezade, V. and Razmi, H. (2026) Eco-Friendly High-Performance Aptasensor for Ultra-Sensitive Methamphetamine Detection in Biofluids Using Carbon Felt Modified by Ti3C2Tx MXene and Silver Nanodendrites. *Talanta*, **298**, Article 129035. https://doi.org/10.1016/j.talanta.2025.129035

[22] Bose, R., Alanazi, A.K., Bhowmik, S., Garai, S., *et al.* (2023) Applications of Graphene and Graphene Oxide as Versatile Sensors: A Brief Review. *Biointerface Research in Applied Chemistry*, **13**, Article 33263.

[23] Magnusson. B. and Örnemark, U. (2014) Eurachem Guide: The Fitness for Purpose of Analytical Methods: A Laboratory Guide to Method Validation and Related Topics. Eurachem.

[24] Ma, M., Yang, X., Ying, X., Shi, C., Jia, Z. and Jia, B. (2023) Applications of Gas Sensing in Food Quality Detection: A Review. *Foods*, **12**, Article 3966. https://doi.org/10.3390/foods12213966

[25] Güneş, G., Can, Z., Arda, A. and Apak, M.R. (2023) Determination of Ketamine Using Melamine-Modified Gold Nanoparticles. *Turkish Journal of Chemistry*, **47**, 1053-

1063. https://doi.org/10.55730/1300-0527.3593

[26] Imas, J.J., Ruiz Zamarreño, C., Zubiate, P., Sanchez-Martín, L., Campión, J. and Matías, I.R. (2020) Optical Biosensors for the Detection of Rheumatoid Arthritis (RA) Biomarkers: A Comprehensive Review. *Sensors*, **20**, Article 6289. https://doi.org/10.3390/s20216289

[27] Prasher, P. and Sharma, M. (2022) Silver Nanoparticles: Synthesis, Functionalization and Applications. Bentham Science Publishers.

[28] Lucas, S.B., Duarte, L.M., Rezende, K.C.A. and Coltro, W.K.T. (2022) Nitrite Determination in Environmental Water Samples Using Microchip Electrophoresis Coupled with Amperometric Detection. *Micromachines*, **13**, Article 1736. https://doi.org/10.3390/mi13101736

[29] Xu, N., Jin, S. and Wang, L. (2020) Metal Nanoparticles-Based Nanoplatforms for Colorimetric Sensing: A Review. *Reviews in Analytical Chemistry*, **40**, 1-11. https://doi.org/10.1515/revac-2021-0122

[30] Uddin, R., Islam, G.M.R., Uddin, M.Z. and Thakur, M.U. (2023) Development and Validation of an Effective and Sensitive Technique for Nitrate Determination in Fruits and Vegetables Using HPLC/PDA. *BMC Chemistry*, **17**, Article No. 105. https://doi.org/10.1186/s13065-023-01008-y

[31] Prasad, S. and Chetty, A.A. (2011) Flow Injection Assessment of Nitrate Contents in Fresh and Cooked Fruits and Vegetables Grown in Fiji. *Journal of Food Science*, **76**, 200-205. https://doi.org/10.1111/j.1750-3841.2011.02346.x

[32] Zhao, S., Tong, J., Li, Y., Sun, J., Bian, C. and Xia, S. (2019) Palladium-Gold Modified Ultramicro Interdigital Array Electrode Chip for Nitrate Detection in Neutral Water. *Micromachines*, **10**, Article 223. https://doi.org/10.3390/mi10040223

[33] Beaton, A.D., Cardwell, C.L., Thomas, R.S., Sieben, V.J., Legiret, F., Waugh, E.M., *et al.* (2012) Lab-on-Chip Measurement of Nitrate and Nitrite for *in Situ* Analysis of Natural Waters. *Environmental Science & Technology*, **46**, 9548-9556. https://doi.org/10.1021/es300419u